



**HAL**  
open science

## Sharing effort in planning human-robot handover tasks

Jim Mainprice, Mamoun Gharbi, Thierry Simeon, Rachid Alami

► **To cite this version:**

Jim Mainprice, Mamoun Gharbi, Thierry Simeon, Rachid Alami. Sharing effort in planning human-robot handover tasks. IEEE RO-MAN: The 21st IEEE International Symposium on Robot and Human Interactive Communication, Sep 2012, Paris, France. hal-01976706

**HAL Id: hal-01976706**

**<https://hal.laas.fr/hal-01976706>**

Submitted on 10 Jan 2019

**HAL** is a multi-disciplinary open access archive for the deposit and dissemination of scientific research documents, whether they are published or not. The documents may come from teaching and research institutions in France or abroad, or from public or private research centers.

L'archive ouverte pluridisciplinaire **HAL**, est destinée au dépôt et à la diffusion de documents scientifiques de niveau recherche, publiés ou non, émanant des établissements d'enseignement et de recherche français ou étrangers, des laboratoires publics ou privés.

# Sharing effort in planning human-robot handover tasks

Jim Mainprice<sup>1,2</sup>, Mamoun Gharbi<sup>1,2</sup>, Thierry Siméon<sup>1,2</sup>, Rachid Alami<sup>1,2</sup>

{jmainpri, magharbi, nic, rachid}@laas.fr

<sup>1</sup>CNRS ; LAAS ; 7 avenue du colonel Roche, F-31077 Toulouse, France

<sup>2</sup>Université de Toulouse; UPS, INSA, INP, ISAE ; LAAS ; F-31077 Toulouse, France

**Abstract**—For a versatile human-assisting mobile-manipulating robot such as the PR2, handing over objects to humans in possibly cluttered workspaces is a key capability. In this paper we investigate the motion planning of handovers while accounting for the human *mobility*. We treat the human motion as part of the planning problem thus enabling to find broader type of handing strategies. We formalize the problem and propose an algorithmic solution taking into account the *HRI constraints* induced by the human receiver presence. Simulation results with the PR2 robot illustrate the efficacy of the approach.

## I. INTRODUCTION

Robots and humans working together in cooperation can accomplish more sophisticated tasks benefiting from the combined power/precision of the robot and the reasoning of the human. This relationship brings new problems and challenges to robotics research.

In this paper we focus on the particular problem of finding good object handover configurations, that is formulated as a special instance of the motion planning problem [5], [11], [12]. We consider robots such as the PR2, with navigation and manipulation capabilities and introduce the notion of "shared effort" in the handover plan.

Human-aware motion planning is a rather active area of research [9], [10], [13], [16], [20]. These works generally use a costmap approach in order to account for the human preferences according to the *proxemics* theory [6]. Other work aim at making humanoid robots motions more human-like [1], [17], [21], [22] to increase the robot-motion legibility. However we are not aware of motion planners that account for the human motions for generating more comfortable robot behaviors.

Human-robot handovers have been studied through several aspects such as relative placement [8], arm motion trajectory and dynamics [18], coordination and signaling [7], human safety, acceptance or comfort. Recently, Edsinger and Kemp, demonstrated in [4] that humans tend to adapt to the robot shape and its limited grasping capacities by selecting handover positions to ease the transfer of the object to be exchanged. In the paper they discuss the importance of geometrical features to be taken into account such as the notion of private space [6] to generate the reaching gestures. They claim that taking into account such constraints would result in more intuitive, more comfortable, and more efficient handovers. Cakmak et al [3] have introduced the notion of *contrast* to design the handover posture. This was motivated by observing that robot poses are often not conveying the

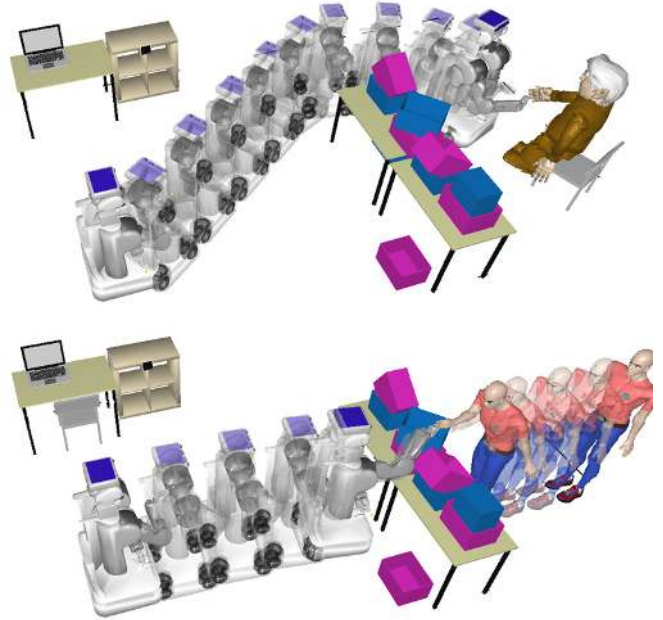


Fig. 1. A young person that is in a hurry to get the object will express more comfort getting the object above the cluttered table while an older person will take the object from the side even with a longer wait.

intent because of the ambiguous boundary between carry and handover postures.

In this work we propose to consider the human motion while planning for robot-human handovers in a workspace possibly cluttered by obstacles. Our aim is to better account for human preferences such as *eagerness* to get the object or *physical capacities*. We introduce a number of criteria for the exchange to be safe, legible and fluent, and propose a formulation of the underlying planning problem. We also introduce a new parameter named *mobility* to balance between "shared effort" and comfort. We have developed an efficient algorithmic solutions to this planning problem. Figure 1 presents an example of a handover task solved by our planner with different settings of the *mobility* parameter.

The paper is organized as follows. Section II gives a formal definition to the handover planning problem. Section III introduces a simple but yet computationally efficient algorithm based on a combination of grid-based and sampling-based methods. Section IV presents the simulation and experimental results obtained using this approach.

## II. THE HUMAN-ROBOT HANDOVER PLANNING PROBLEM

In this section we propose a formal definition of the handover planning problem. We first introduce the input and output of the problem, then we define the search space along with the feasibility and interaction constraints to be taken into account.

### A. Inputs and outputs

In order to account for the human's motion we consider motion plans that are composed of two paths: the giver's and the receiver's paths that take them from their initial posture to a feasible handover goal posture.

Formally the inputs of the problem are the initial configurations of the robot  $q_r^{init}$  and of the human  $q_h^{init}$ . The problem also takes as input their kinematic model and the representation of the workspace  $W$ . The output plan will consist of the two paths  $\tau_r$  and  $\tau_h$  represented as parametric curves in their respective configuration space.

Next, we define the handover configuration space as the space of all feasible handover postures and further present a set of properties that are used to assess the quality of the output plan in terms of interaction constraints.

### B. The handover configuration space

Let us consider the configuration space formed by the cartesian product between the robot configuration space  $C_r$  and the human configuration space  $C_h$ :

$$C = C_r \times C_h$$

The configuration space  $C$  contains all configurations allowed by the kinematics of both the robot and the human. Thus solving the handover problem implies to find a handover configuration  $q_{hand} = (q_r, q_h) \in C$ . The configuration  $q_{hand}$  belongs to a feasible subspace  $C_{feas} \in C$ . This subspace is a restriction of  $C$  regarding the constraints listed below:

a) *Collision free*: at the handing configuration  $q_{hand}$ , the robot and the human have to be collision free regarding self collision, collision with obstacles and with each other. This subspace is named  $C_{free}$ .

b) *Reachability*: at the handing configuration  $q_{hand}$ , the object to be exchanged has to be reachable by both partners i.e. the gripper of the robot and the hand of the human must grasp the object. This subspace is named  $C_{reach}$ .

c) *Stability*: at the handing configuration  $q_{hand}$ , the robot and the human have to be stable regarding newton law of mechanics. This subspace is named  $C_{stab}$ .

d) *Accessibility*: this constraint corresponds to the existence of a collision free path between the handing posture  $q_{hand}$  and the initial configuration  $q_{init} = (q_r^{init}, q_h^{init})$ . The set of handing configuration accessible from  $q_{init}$  defines the subspace named  $C_{access}$ .

The set of all feasible handover configurations  $C_{feas}$  is the intersection of these four subspaces:

$$C_{feas} = C_{free} \cap C_{reach} \cap C_{stab} \cap C_{access}.$$

$C_{feas}$  only restricts the configuration space to feasible handover motions where the robot and the human can meet in a handing posture. In this possibly large subspace of  $C$  many configurations may be undesirable because they do not respect social protocols or do not consider explicitly human preferences. In the next subsection we detail some important properties that have to be accounted for in order to generate valid human-robot handovers regarding intuitive social rules and the more formal *proxemics* theory.

### C. HRI constraints

In order to account for the safety of the interaction and the legibility of the robot's intentions, we have introduced in [20] and [13] a set of HRI constraints that rely on notions from the *proxemics* theory [6] as well as user studies such as [8]. These constraints have been introduced and used in [20] to generate navigation human-aware motions. They have also been used in [13] to generate comfortable handover motions in cluttered environments. Each interaction constraint is associated to a function that assesses the constraint. These constraints can be summarized in three sets.

First, we consider comfort constraints that prevent generating uncomfortable configurations. They integrate criteria such as robot proximity [6], robot visibility [8] to limit the effect of surprise and musculoskeletal comfort of a given posture [14]. We referred to the corresponding cost as  $c_{comf}$  in the rest of the paper.

Second, we consider motion constraints to generate reasonable effort on the human side. These constraints depend on two parameters: displacement, and standing. The length of the path  $\tau_h$  that the human will have to walk and whether the human needs to stand up are used to assess this constraint. We will refer to the corresponding cost as  $c_{mot}$ .

Finally, we also account for fluency constraints, limiting the total duration of the handover, and favoring efficient plans. For this, we consider a cost  $c_{length}$  related to the maximum value of the time taken by either the robot or the human to reach the handover configuration.

Some of these desired properties such as the human displacement and the action duration may contradict one another. To balance the impact of the different properties on the output plan, we introduce a mobility parameter reflecting the giver's physical capabilities and his eagerness to obtain the object.

Indeed, the handover duration may generate discomfort if it does not match with the human possible *eagerness* or *urgency* to get the object. High mobility values will balance motion and comfort constraints to favor quicker plans, resulting in the final cost defined as :

$$c = (c_{mot} + c_{comf}) * (1 - m) + c_{length} * m$$

where  $m \in [0 1]$  is the mobility factor. As explained in next section these interaction constraints and their corresponding cost functions are evaluated during the planning process and are combined together according to the human preferences modeled by the *mobility* parameter.

### III. ALGORITHM

This section presents the handover planner that was developed to compute human-robot handovers while accounting for the interaction constraints introduced above. The approach relies on a combination of grid-based and sampling-based algorithms that consider the workspace obstacles and the kinematics models of both the human and the robot. After some grid based preprocessing, the method consists of iteratively sampling feasible handover configurations, evaluating their cost and finally returning the minimal cost plan obtained.

The main steps of the handover planner are sketched in Algorithm 1. An initialization phase, called `initGrids`, computes the accessibility of the human and the robot in the plane which are stored in two planar grids. These grids also contain the navigation distance to the robot and human initial position (see Figure 2). In this phase, two preselected sets of human-robot handover configurations are also loaded for a standing and sitting human (see Figure 3).

After the initialization phase, each iteration consists of computing a handover configuration  $q_{hand}$  that encodes for the robot and the human DoFs.

The navigation parameters  $p = (x, y, \theta)$  of the human at  $q_{hand}$ , are first generated in the `SampleHumanPos` function by sampling a random position in the human accessible space. The navigation path of the human  $\tau_h$  to reach this position is computed by using a standard technique [11] consisting of descending the distance gradient in the preprocessed human grid. Note that the robot path  $\tau_r$  is computed similarly by descending the distance gradient in the robot grid.

The position  $p$  is then transformed into to a fully specified handover configuration  $q_{hand}$  in the `BestFeasibleConf` function that iterates through the set of preselected human-robot handing configurations loaded in the initialization phase. Then if no feasible robot path  $\tau_r$  is found between the robot initial position and the handover configuration the algorithm returns to step one. Otherwise the cost of the solution plan is evaluated and stored if it improves the minimum cost solution found by previously computed handover plans.

The method loops over these steps until the stopping criterion is satisfied. In the current implementation the stopping conditions combines two stopping criteria : maximum time or a minimal improvement of the best current solution. The final robot path  $\tau_r$  consists of a set of way points corresponding to the trasversed cells centers interpolated by straight lines. The orientation  $\theta$  along  $\tau_r$  is selected implicitly by facing the robot to the next way point.

In the next subsections we further detail the processing done during the initialization phase and the three steps of the algorithm. We also describe some additional pre-processing that can be done to speed-up the sampling of constrained handover solutions.

---

#### Algorithm 1: Computing handover plans

---

```

input   : Human initial position :  $p_h$ 
           : Robot initial position :  $p_r$ 
           : Mobility of the human :  $m$ 
output  : The human and robot handover conf :  $q_{hand}$ 
           : Human path :  $\tau_h$ 
           : Robot path :  $\tau_r$ 

begin
   $cost^{best} \leftarrow \infty$ 
   $G \leftarrow \text{initGrids}(p_h, p_r, m)$ ;
  while StopCondition() do
     $p \leftarrow \text{SampleHumanPos}()$ 
     $\tau_h \leftarrow \text{DescendOnHumanGrid}(p)$ 
     $q_{hand} \leftarrow \text{BestFeasibleConf}(p)$ 
    if  $q_{hand} == NULL$  then
      continue
     $p_{rob} \leftarrow \text{GetRobotPos}(q_{hand})$ 
     $\tau_r \leftarrow \text{DescendOnRobotGrid}(p_{rob})$ 
    if not  $\tau_r == NULL$  then
      continue
     $cost \leftarrow \text{ComputeCost}(m, \tau_h, \tau_r, q_{hand})$ 
    if  $cost > cost^{best}$  then
      continue
    else
       $cost^{best} \leftarrow cost$ 
      StoreBest( $q_{hand}, \tau_h, \tau_r$ )
  return
end

```

---

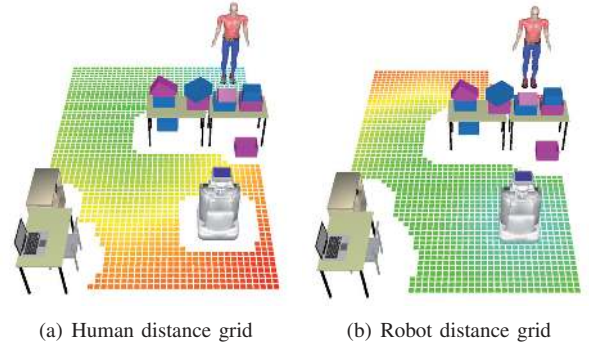


Fig. 2. The distance propagation (a) is human centered and (b) is robot centered. the green cells correspond to nearest positions, and the red the farthest.

#### A. Distance propagation and initialization

In order to facilitate the computation of feasible handover configurations and the cost evaluation of those solutions, the method integrates a precomputing phase in which two dimensional grids are constructed and processed. Two grids, depicted on Figure 2, one for the robot and one for the human, provide an approximation of the free-space and the navigation distance to the initial position. This enables to determine which region of the workspace are accessible to the human and the robot at a very low computational cost.

The free-space grids are computed using bounding cylinders of the robot and the human in resting postures. The resting postures, also depicted in Figure 2, correspond to



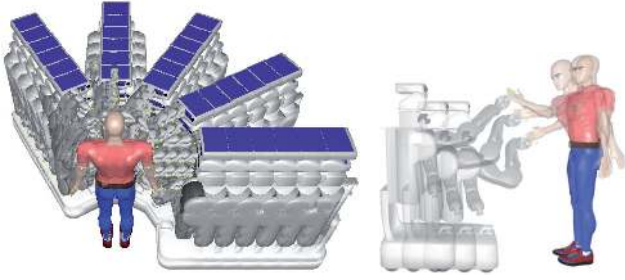


Fig. 3. The preselected configurations of the robot relative to the human standing (similar configurations are generated for the human sitting).

navigation configuration of the arms. A cell is marked as free if when placed at its center, the corresponding bounding cylinder does not overlap with the workspace obstacles.

The accessible space and the navigation distance to the initial position of a cell are simultaneously computed with a standard wave propagation technique. Figure 2 shows the propagated distance of the robot and the human from their initial position, where green cells are close to the initial position and red cells are far.

The initialization phase also loads a set of predefined handing configurations illustrated in Figure 3. These human-robot handover configurations are named  $Q_{HR}$  in the rest of the paper. They are selected offline and do not depend on the workspace nor on the absolute position of the human and the robot. Thus each configuration is defined relatively to the human position and consists of the human's and the robot's arm DoFs. The selection of these configurations can be done by sampling relative human-robot positions and using them to compute the associated handover configurations.

### B. Sampling human positions

The first step of each iteration consists of sampling a human position and orientation  $p = (x, y, \theta)$  inside the accessible space stored in the pre-processed grid. In order to sample this triplet a cell is selected then a point is sampled inside the cell and finally an orientation is randomly sampled.

Since each sampled position  $p$  leads to one and one only best handover plan, it is important to sample the positions that yield better solutions. We provide in Section III-D, two enhancements of the preprocessing phase to bias both the selection of the cell and the orientation of the human.

### C. Returning the best feasible configuration

The configurations  $Q_{HR}$  illustrated in Figure 3 are sorted according to the  $c_{com,f}$  cost (see Section II-C). When searching for the best feasible handover configuration at human position  $p$ , the first feasible configuration is selected (i.e. collision free and accessible to the robot).

This process enables to find constrained handover configurations, e.g. a small slot in a wall that separates disconnected parts of the workspace. Moreover, since the configurations are sorted, the best configuration regarding comfort cost is quickly determined without recomputing cost.

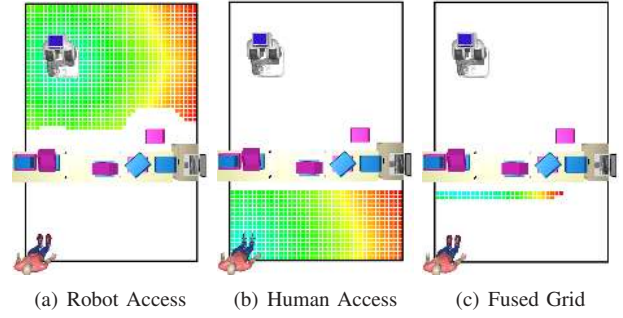


Fig. 4. The human and the robot lie in separated part of a workspace, parted in two by a table. The accessible space of the robot (a) and human (b) and the fused grid (c) are computed.

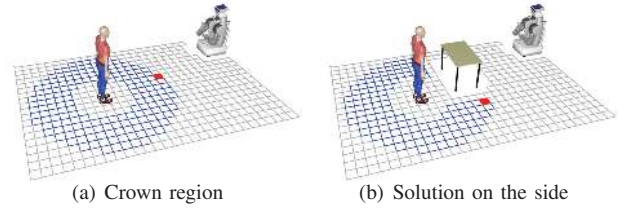


Fig. 5. The estimated handover positions of the robot, feasible (in blue) and closest feasible  $cell_{min}$  (in red) for a given human position according to the reaching capabilities of the human and the robot.

### D. Reduce the search space and biasing sampling

When the human and the robot lie in separated parts of the workspace, such depicted in Figure 4, the algorithm samples the human accessible space without considering the robot accessibility and reaching capacity. The human direction is also sampled randomly which is often away from the robot approaching direction.

In order to speed-up and ameliorate the generation of feasible handover configurations we propose two enhancements to the basic version. First, we construct a smaller fused grid which contains only human cells that can lead to potentially valid handovers by discarding cells that are unreachable to the robot. Secondly, a value which approximates the total cost of the candidate handover solution is precomputed and stored in the grid. Human position sampling is then biased to low cost regions of the accessible space stored in the fused. The sampling of the human direction is also biased to an estimate of the robot approaching direction.

1) *Fused grid*: To generate the fused grid of the human and robot accessible space the minimal and maximal human-robot distances in the preselected set of handing configuration  $Q_{HR}$  are computed. These  $min$  and  $max$  values are used to define a crown region around the human such as illustrated in Figure 5. Then each accessible cell in the human grid which crown region does not overlap any cell in the robot grid (i.e. that can not yield a valid handover configuration) are suppressed from the human grid.

Hence, by discarding the cells that are not within reaching distance from the robot accessible space a smaller fused grid is obtain, such as depicted in Figure 4.c. Note that the fused grid does not account for 3D collision checking which is

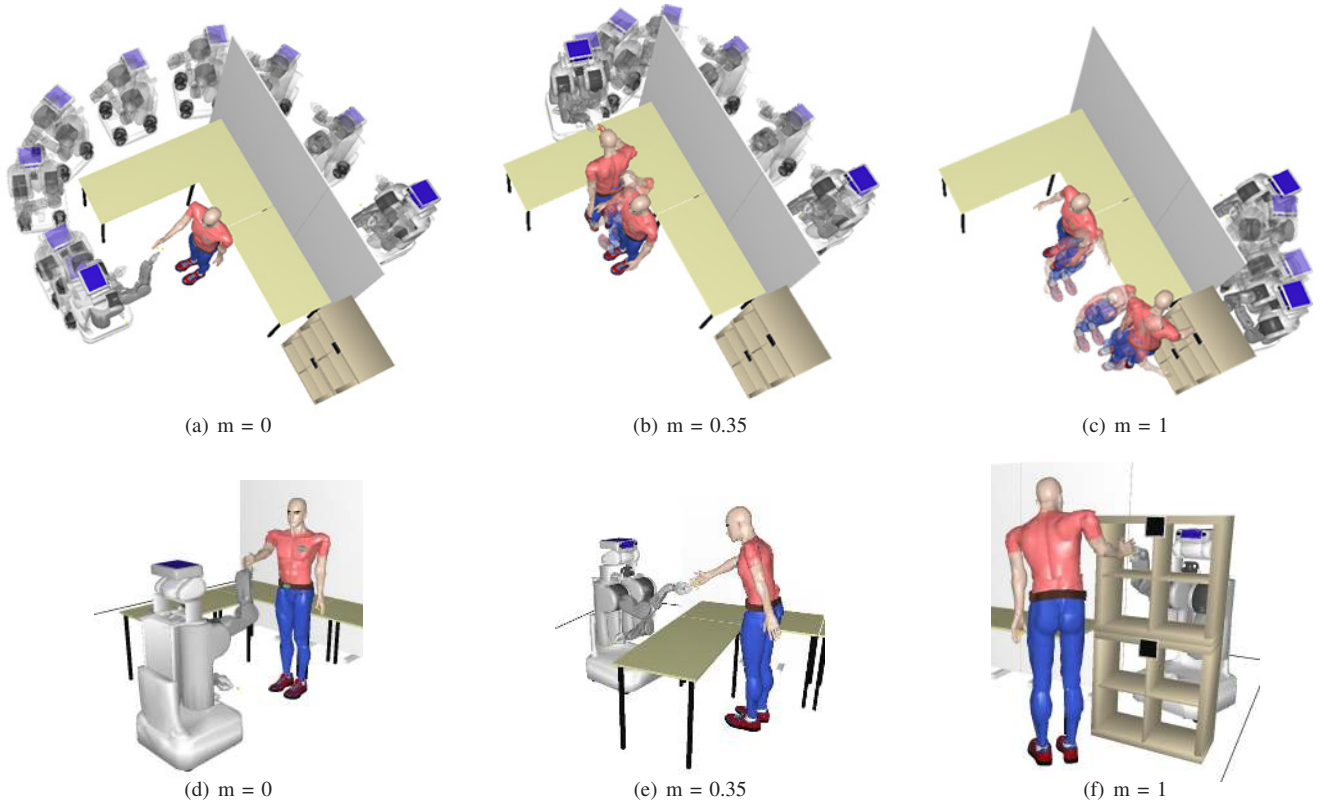


Fig. 6. Three values of the *mobility* parameters are used to generate three handover strategies. The first three pictures depict the resulting trajectories while the three bottom pictures show the final handover configuration that accounts for the 3D obstacles.

performed in the exploration phase.

2) *Bias sampling*: In order to bias the sampling of human position to candidates that will yield better handover configurations, each cell in the fused grid is filled with path length cost and motion length cost as follows:

$$c_B = c_{mot} * (1 - m) + c_{length} * m$$

where  $m$  is the mobility parameter, this value  $c_B$  approximates the final  $c$  presented in Section II-C that is used to evaluate the quality of the candidate handover solution.

In order to bias the human direction sampling, the valid cell that minimizes the robot motion from its initial position to the crown region (in red in Figure 5) is stored in the fused grid. When sampling  $\theta$ , directions facing this cell are favored.

Next section provides simulation results of this algorithm with different settings of the  $m$  parameter. We also present a user study that has been conducted to validate this approach.

#### IV. RESULTS

In this section we report the capability of the algorithm to find handover plans in workspaces containing home furniture such as tables and shelves. We report the strategies produced by the planner using different values of  $m$  and the convergence rate of the algorithm when using different pre-processing variants and their sampling schemes. We also discuss discretization issues.

In order to assess its performance, the algorithm has been implemented, along with test environments, into the path planning software *Move3D* [19] and simulation were performed on a 2.26GHz INTEL processor.

##### A. Influence of the mobility parameter

Figure 6 shows three handover strategies that have been computed for the same problem using three values of the  $m$  parameter. For low values of  $m$ , the human is supposedly less involved, asked as little effort as possible, on the contrary high values of  $m$  supposedly require more effort and participation of the human resulting in quicker handover strategies.

- $m = 0$ : Generates a long path for the robot to reach the handover position and the human does not move.
- $m = 0.35$ : A shorter robot path to a feasible handover position over the table is allowed by small displacement of the human.
- $m = 1$ : Shared effort between robot and human enables a constrained handover position through the shelves.

Note that the planner is able to find different feasible handover positions for the same initial position of the human and the robot in the same environment. The resulting plan accounts for the feasibility of the handover position and motion using the 3D models of the human and the robot even though planning of navigation motion is performed in 2D cartesian space.

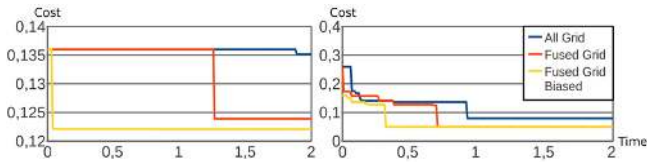


Fig. 7. Unique convergence curve, with two settings of  $m$ , using the three pre-processing variants yielding three sampling strategies over the scenario depicted in Figure 6 ( $m=0.35$  right,  $m=1$  left)

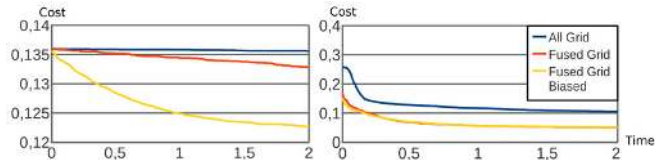


Fig. 8. Averaged convergence curve over 300 runs, with the same settings as shown in Figure 7 ( $m=0.35$  right,  $m=1$  left)

### B. Performance of preprocessing variants

Figure 7 shows the cost improvement over two seconds on a single run corresponding to approximately one thousand sampled positions and five hundred fully tested handover strategies. The figure illustrates the interest of the proposed fused grids and bias variants.

The simplest case ( $m=0$ ) is not shown in a figure since all variants converge to the displayed solution after a couple of iterations. However for the two more complex cases the basic pre-processing shows difficulty to find handover over the table ( $m=0.35$ ) or through shelves ( $m=1$ ). In order to generate more direct (and lower cost) handovers the basic version requires much more iterations than the other variants. The basic method keeps sampling handover configurations in the free space similar to the ones shown in Figure 6.a and 6.d, but placed elsewhere in the free-space.

Thanks to fused grids the algorithm generates more samples on the boundary of the free space (close to the tables) and thanks to bias it discovers more easily the solution through the shelves. Figure 8 shows similar results averaged over 300 runs of the planner which confirms these results. In average a good quality solution is obtained in less than 1 sec with the fused grid and bias sampling preprocessing.

### C. Influence of discretization

Figure 9 shows for the case  $m=1$  that the grid size has little influence on the performance of the handover sampling stage. The influence is limited to the preprocessing stage for which distance propagation and fused grid computation depend on the resolution. Note that the preprocessing is problem dependent (initial position of the robot and the human) and has to be performed for each query.

In terms of preprocessing time, the basic preprocessing requires  $200msec$  (resp.  $660msec$ ) for a resolution of 20cm (resp. 10cm) and the additional cost of computing the fused grid is  $68msec$  (resp.  $1109msec$ ). Thus, using a resolution of 20cm, the preprocessing stays below 1sec, however it may become higher for discretization below 10cm.

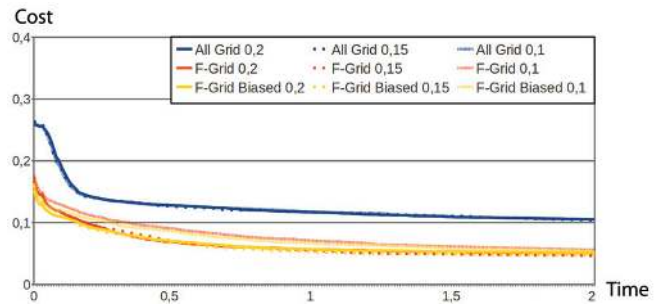


Fig. 9. Averaged convergence over 300 runs on the scenario of Figure 6 with  $m=1$ . Three distinct grid sizes 10, 15 and 20 cm are superposed

The performance above tend to indicate that this approach could be used to dynamically adapt the computed handover motion plan during execution in order to account for possible human motions or to adapt the *mobility* factor if the human motion does not look compatible with the proposed handover location.

## V. IMPLEMENTATION AND USER STUDY

We have conducted an HRI experiment confronting the participants to choices of handover configurations that are outputs of our planner: the shortest-time feasible plan at the cost of substantial effort asked to the human, or the plan that minimizes the human effort, at the cost of low global performance.

The handover planner has been implemented on the PR2 robot. The trajectories of the arm were planned within *Move3D* and executed with a *SoftMotion* controller [2] limiting the motion in jerk, accelerations and velocity. The moving objects were localized with a tag detection module based on ARToolKit [15]. We made use of an external Kinect to localize humans in the scene we also controlled the head of the robot and diffused sound on the robot speakers.

Figure 10 shows two participants being handed the object in two distinct settings of the  $m$  parameter. The 34 subjects recruited at the LAAS-CNRS in Toulouse, France were faced with one handover only. At their arrival, the subjects were briefed before the interaction, the handover was video recorded and the participants were finally handed a survey.

We expected that accounting for the human *mobility* resulted in more fluent and more efficient hand-overs. We also expected that the *mobility* of the human receiver depended on the task and intrinsic parameters. Hence we hypothesized that appropriate matching and tuning of the *mobility* parameter regarding the human preferences would result in a smoother and a more comfortable human-robot interaction.

The environment was built such that to put the planner in a "substantially difficult" situation: save time at the cost of human effort and unease to perform the task. The robot was able too build a shared plan where it hands over the object through a hole that is not large enough to allow the robot nor the human to cross.

The participants were assigned to four distinct cases.



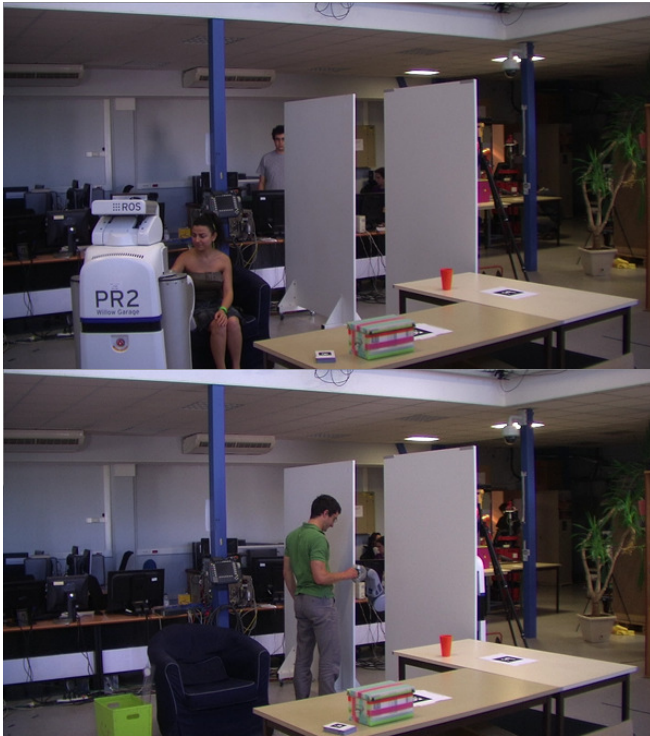


Fig. 10. Two participants of the HRI handover experiment. The first one is handed the object with a low mobility and the second one with a high mobility.

- Shortest hand-over plan with chronometer
- Shortest hand-over plan with 'sudoku'
- Less effort hand-over plan with chronometer
- Less effort hand-over plan with 'sudoku'

Where sudoku and chronometer corresponded to two distinct tasks, that supposedly increased or decreased the mobility of the participant. Objective and subjective measures (timing and survey) were used to validate the hypothesis. The results lent support to the hypothesized role of the mobility parameters and also corroborated the *proxemics* theory which has been the basis of this work.

## VI. CONCLUSIONS AND FUTURE WORKS

This paper was motivated by the need for robot to plan for handover motions in possibly cluttered scenes while accounting for the human safety and comfort. Hence we have introduced a new type of path planning problem that we call the handover planning problem. The novelty of this approach is to account for human motions for planning the robot motion and the associated handover configuration. We have formalized this problem and proposed a simple but efficient algorithm. This algorithm is based on a combination of simple sampling-based and grid-based techniques providing a time efficient solution. In order to account for the human motion we introduce a new parameter to qualify the human state we call *mobility*.

We have used this framework to compute handover solution while considering the human static. However the fast convergence times indicate that it can be used to dynamically

adapt handover configuration while the human is moving. In future work we also aim to further formalize and generalize this approach to new human-robot interactions problems. We also plan to perform a more realistic user-study accounting for the human motion during execution of planned motion.

## VII. ACKNOWLEDGMENTS

This work has been conducted within the EU SAPHARI project (<http://www.saphari.eu/>) funded by the E.C. Division FP7-IST under Contract ICT-287513.

## REFERENCES

- [1] T. Asfour and R. Dillmann. Human-like motion of a humanoid robot arm based on closed-form solution of the inverse kinematics problem. In *IEEE/RSJ Int. Conf. on Intel. Rob. And Sys (IROS)*, 2003.
- [2] X. Broquère, D. Sidobre, and I. Herrera-Aguilar. Soft motion trajectory planner for service manipulator robot. In *IEEE/RSJ Int. Conf. on Intel. Rob. And Sys (IROS)*, 2008.
- [3] M. Cakmak, S.S. Srinivasa, M.K. Lee, S. Kiesler, and J. Forlizzi. Using spatial and temporal contrast for fluent robot-human hand-overs. *ACM*, 2011.
- [4] A. Edsinger and C.C. Kemp. Human-robot interaction for cooperative manipulation: Handing objects to one another. In *RO-MAN 2007*. IEEE, 2008.
- [5] H. Choset et al. *Principles of robot motion: theory, algorithms, and implementation*. The MIT Press, 2005.
- [6] Edward T. Hall. A system for the notation of proxemic behavior. *American anthropologist*, 1963.
- [7] M. Huber, M. Rickert, A. Knoll, T. Brandt, and S. Glasauer. Human-robot interaction in handing-over tasks. In *RO-MAN*. IEEE, 2008.
- [8] K. L. Koay, E. Akin Sisbot, D. A. Syrdal, M. L. Walters, K. Dautenhahn, and R. Alami. Exploratory study of a robot approaching a person in the context of handling over an object. In *AAAI*, Palo Alto, CA, USA, 2007.
- [9] D. Kulic and E. Croft. Physiological and subjective responses to articulated robot motion. *Robotica*, 2007.
- [10] C.P. Lam, C.T. Chou, K.H. Chiang, and L.C. Fu. Human-Centered Robot Navigation, Towards a Harmoniously Human-Robot Coexisting Environment. *Robotics, IEEE Transactions on*, 2010.
- [11] J.C. Latombe. *Robot motion planning*. Springer, 1991.
- [12] S.M. LaValle. *Planning algorithms*. Cambridge Univ Pr, 2006.
- [13] J. Mainprice, E.A. Sisbot, L. Jaillet, J Cortés, T. Siméon, and R. Alami. Planning Human-aware motions using a sampling-based costmap planner. In *IEEE Int. Conf. Robot. And Autom. (ICRA)*, 2011.
- [14] R.T. Marler, S. Rahmatalla, M. Shanahan, and K. Abdel-Malek. A new discomfort function for optimization-based posture prediction. 2005.
- [15] S. Prince, A.D. Cheok, F. Farbiz, T. Williamson, N. Johnson, M. Billingham, and H. Kato. 3d live: Real time captured content for mixed reality. In *ISMAR 2002*.
- [16] L. Scandolo and T. Fraichard. An Anthropomorphic Navigation Scheme for Dynamic Scenarios. In *IEEE Int. Conf. Robot. And Autom. (ICRA)*, 2011.
- [17] L. Sentis and O. Khatib. A whole-body control framework for humanoids operating in human environments. In *IEEE Int. Conf. Robot. And Autom. (ICRA)*, 2006.
- [18] S. Shibata, K. Tanaka, and A. Shimizu. Experimental analysis of handing over. In *Robot and Human Communication, RO-MAN, Proceedings., 4th IEEE International Workshop on*, 1995.
- [19] T. Simeon, JP Laumond, and F. Lamiroux. Move3D: a generic platform for path planning. In *4th Int. Symp. on Assembly and Task Planning*, pages 25–30. Citeseer, 2001.
- [20] E. A. Sisbot, L. F. Marin-Urias, R. Alami, and T. Siméon. Human aware mobile robot motion planner. *IEEE Transactions on Robotics*, 2007.
- [21] M. Toussaint, M. Gienger, and C. Goerick. Optimization of sequential attractor-based movement for compact behaviour generation. In *Humanoid Robots, 7th IEEE International Conference on*, 2007.
- [22] F. Zacharias, C. Schlette, F. Schmidt, C. Borst, J. Rossmann, and G. Hirzinger. Making planned paths look more humanlike in humanoid robot manipulation planning. In *IEEE Intl. Conf. on on Robotics and Automation (ICRA)*, 2011.